Article no. 14

THE CIVIL ENGINEERING JOURNAL 3-2016

OPTIMIZATION OF THE TEMPERATURE CONTROL SCHEME FOR ROLLER COMPACTED CONCRETE DAMS BASED ON FINITE ELEMENT AND SENSITIVITY ANALYSIS METHODS

Huawei Zhou [1,2], Yihong Zhou [1,2,3], Chunju Zhao [2,3], Zhipeng Liang [4]*

[1] *School of Water Resources and Hydropower Engineering, Wuhan University, Wuhan, 430072, China*
[2] *College of Hydraulic and Environmental Engineering, China Three Gorges University, Yichang, 443002, China*
[3] *Hubei Key Laboratory of Construction and Management in Hydropower Engineering, China Three Gorges University, Yichang 443002, China*
[4] *College of Mechanical and Power Engineering, China Three Gorges University, Yichang, 443002, China*

ABSTRACT

Achieving an effective combination of various temperature control measures is critical for temperature control and crack prevention of concrete dams. This paper presents a procedure for optimizing the temperature control scheme of roller compacted concrete (RCC) dams that couples the finite element method (FEM) with a sensitivity analysis method. In this study, seven temperature control schemes are defined according to variations in three temperature control measures: concrete placement temperature, water-pipe cooling time, and thermal insulation layer thickness. FEM is employed to simulate the equivalent temperature field and temperature stress field obtained under each of the seven designed temperature control schemes for a typical overflow dam monolith based on the actual characteristics of a RCC dam located in southwestern China. A sensitivity analysis is subsequently conducted to investigate the degree of influence each of the three temperature control measures has on the temperature field and temperature tensile stress field of the dam. Results show that the placement temperature has a substantial influence on the maximum temperature and tensile stress of the dam, and that the placement temperature cannot exceed 15 °C. The water-pipe cooling time and thermal insulation layer thickness have little influence on the maximum temperature, but both demonstrate a substantial influence on the maximum tensile stress of the dam. The thermal insulation thickness is significant for reducing the probability of cracking as a result of high thermal stress, and the maximum tensile stress can be controlled under the specification limit with a thermal insulation layer thickness of 10 cm. Finally, an optimized temperature control scheme for crack prevention is obtained based on the analysis results.

KEYWORDS

Concrete dam, Temperature control parameters, Finite element method, Numerical simulation, Sensitivity analysis

INTRODUCTION

During the construction of a roller compacted concrete (RCC) dam, large quantities of concrete are employed to form a monolithic mass concrete structure [1]. Heat generated by the hydration of cement leads to a rising temperature in the dam body, and, owing to its massiveness, several years are required for a concrete dam to attain a stable temperature after a peak temperature

is reached [2]. Such variations in the temperature of concrete dams usually lead to cracking, which greatly impacts the quality and safety of concrete dams. To address this substantial problem, various concrete temperature control measures, such as water-pipe cooling, concrete pre-cooling, surface heat preservation, and thin layer placement, are typically employed in the construction process. Nevertheless, thermal cracking still often occurs due to an ineffective combination of these measures.

Numerous studies have been published regarding temperature control scheme design for RCC dams based on numerical analysis methods, which have proven to be effective for the verification of temperature control measures. Chen et al. [3] developed a three-dimensional (3-D) finite element relocating mesh method (TDFERMM) for conducting computational simulation analysis of the temperature and thermal stress distributions in an RCC dam. Malkawi et al. [4] conducted a coupled thermal-structural analysis using both a two-dimensional (2-D) and a 3-D finite element method (FEM). Xie et al. [5] simulated different types of impervious layers with different thicknesses using TDFERMM for the third grader RCC dam. A 2-D finite element code was developed and verified by Noorzaei et al. [6] for the thermal and structural analysis of RCC dams. Jaafar et al. [7] studied the impact of concrete placement schedules on the thermal response of RCC dams with a finite element based computer code. Chen et al. [8] developed a thermal algorithm based on the composite element method (CEM) for massive concrete structures containing lift joints. Teixeira et al. [9] conducted computational studies using a hybrid finite element formulation for cement hydration in concrete structures. Su et al. [10] calculated the temperature stress for high RCC arch dams mixed with MgO based on FEM. Gaspar et al. [11] proposed a probabilistic thermal model to propagate the uncertainties of some of the physical properties of RCCs, and analyzed the influence of parameters with random characteristics. These studies have mainly focused on improving the simulation method employed for computing the temperature and temperature stress fields of concrete dams, whereas few scholars have considered methods for achieving an optimized employment of various temperature control measures.

Various temperature control measures have been widely used in the construction process of concrete dams for crack prevention, although the degrees to which the different measures influence the temperature and temperature stress fields are not equivalent. Establishing the governing factors by which these measures influence the temperature control effect is critical for achieving an effective combination of these measures in the construction organization design and management of a concrete gravity dam.

In this study, a sensitivity analysis of three temperature control measures, selected as concrete placement temperature, water-pipe cooling time, and thermal insulation layer thickness, is performed based on 3-D FEM simulation of the equivalent temperature field and temperature stress field of a model dam. Seven temperature control schemes are defined according to variations in three temperature control measures: concrete placement temperature, water-pipe cooling time, and thermal insulation layer thickness. The purpose of this study is to determine the degree to which the three temperature control measures influence the temperature and temperature tensile stress fields of an RCC dam, and to obtain an optimized temperature control scheme for crack prevention.

METHODOLOGY

Calculation theory of temperature field

The equation of heat conduction considering the effect of water-pipe cooling can be expressed as follows [12].

$$\frac{\partial T}{\partial \tau} = a\left(\frac{\partial^2 T}{\partial x^2} + \frac{\partial^2 T}{\partial y^2} + \frac{\partial^2 T}{\partial z^2}\right) + \frac{Q}{c\rho} \quad (1)$$

where T is the concrete temperature (°C); τ is the time (h); a is the thermal diffusivity coefficient of concrete, given as $a = \lambda / c\rho$ (m²/h); Q is the heat generation rate per volume (kJ/(m³·h)); λ is the thermal conductivity coefficient (kJ/(m·h·°C)); c is the specific heat (kJ/(kg·°C)); and ρ is the material density (kg/m³).

The initial condition is given in terms of standard Cartesian coordinates and time as follows.

$$T(x, y, z, 0) = T_0(x, y, z) \tag{2}$$

Three boundary conditions must be considered during calculation of the temperature field. The first boundary condition is that the surface temperature is a function of time, which is given as

$$T_s(\tau) = f(\tau) \tag{3}$$

The second boundary condition is that the heat flux across the surface is a known function of time, and is given as

$$-\lambda \frac{\partial T}{\partial n} = f(\tau) \tag{4}$$

The adiabatic boundary condition $\partial T / \partial n = 0$ can be obtained by substituting $f(\tau) = 0$ into Eq. (4).

The third boundary condition is that the concrete surface is in contact with the air, which can be expressed as

$$-\lambda \frac{\partial T}{\partial n} = \beta (T_s - T_a) \tag{5}$$

where $T_0(x, y, z)$ is the initial temperature; T_s the surface temperature; n is the surface external normal direction; β is the surface conductance (kJ/(m²·h·°C)); and T_a is the air temperature.

Calculation theory of temperature stress with FEM

The elastic modulus and creep of concrete both vary with respect time, and an incremental method is used with τ divided into a series of time increments $\Delta\tau_n$ ($\Delta\tau_n = \tau_n - \tau_{n-1}$, n=1, 2, 3…), as shown in Figure 1.

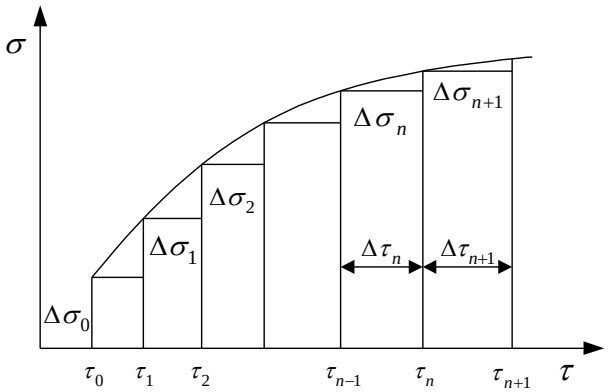

Fig. 1. - Incremental method for calculating the stress

The total strain increment within $\Delta\tau_n$ is

$$\{\Delta\varepsilon_n\} = \{\varepsilon(t_n)\} - \{\varepsilon(t_{n-1})\} = \{\Delta\varepsilon_n^e\} + \{\Delta\varepsilon_n^c\} + \{\Delta\varepsilon_n^T\} + \{\Delta\varepsilon_n^g\} + \{\Delta\varepsilon_n^s\} \tag{6}$$

where $\{\Delta\varepsilon_n^e\}$ is the elastic strain increment; $\{\Delta\varepsilon_n^c\}$ is the creep strain increment; $\{\Delta\varepsilon_n^T\}$ is the temperature strain increment; $\{\Delta\varepsilon_n^g\}$ is the self-grown volume strain increment; and $\{\Delta\varepsilon_n^s\}$ is the dry-shrinkage strain increment.

The relationship between $\{\Delta\sigma_n\}$ and $\{\Delta\varepsilon_n^e\}$ is

$$\{\Delta\sigma_n\} = [D]\{\Delta\varepsilon_n^e\} \tag{7}$$

where $\{\Delta\sigma_n\}$ is the stress increment within the time $\Delta\tau_n$; $[D]$ is the elastic matrix.

The following equation can be obtained by substituting Eq. (6) into Eq. (7).

$$\{\Delta\sigma_n\} = [D](\{\Delta\varepsilon_n\} - \{\Delta\varepsilon_n^c\} - \{\Delta\varepsilon_n^T\} - \{\Delta\varepsilon_n^g\} - \{\Delta\varepsilon_n^s\}) \tag{8}$$

The element nodal forces increment $\{\Delta F_n\}$ within $\Delta\tau_n$ is given by

$$\{\Delta F_n\} = \iiint [B]^T \{\Delta\sigma_n\} dxdydz \tag{9}$$

where $\{\Delta F_n\}$ is the nodal force increment within $\Delta\tau_n$; $[B]$ is the transition matrix of element; *T* represents the transpose of the matrix. Substituting $\{\Delta\sigma_n\}$ expressed by Eq. (8) and $\{\Delta\varepsilon_n\} = [B] \times \{\Delta\delta_n\}$ into the above equation yields

$$\iiint [B]^T [D][B]\{\Delta\delta_n\} dxdydz = \{\Delta F_n\} + \iiint [B]^T [D](\{\Delta\varepsilon_n^c\} + \{\Delta\varepsilon_n^T\} + \{\Delta\varepsilon_n^g\} + \{\Delta\varepsilon_n^s\}) dxdydz \tag{10}$$

where $\{\Delta\delta_n\}$ is the displacement increment of element nodal.

If only considering the temperature load, the following equations are obtained when the exterior loads $\{\Delta F_n\}$ are equal to zero.

$$[K]^e = \iiint [B]^T [D][B] dxdydz \tag{11}$$

$$\{\Delta P_n^c\}^e = \iiint [B]^T [D]\{\Delta\varepsilon_n^c\} dxdydz \tag{12}$$

$$\{\Delta P_n^T\}^e = \iiint [B]^T [D]\{\Delta\varepsilon_n^T\} dxdydz \tag{13}$$

$$\{\Delta P_n^g\}^e = \iiint [B]^T [D]\{\Delta\varepsilon_n^g\} dxdydz \tag{14}$$

$$\{\Delta P_n^s\}^e = \iiint [B]^T [D]\{\Delta\varepsilon_n^s\} dxdydz \tag{15}$$

where $[K]^e$ is the element stiffness matrix; $\{\Delta P_n^c\}^e$ is the nodal load increment due to creep strain; $\{\Delta P_n^T\}^e$ is the nodal load increment due to temperature change; $\{\Delta P_n^g\}^e$ is the nodal load increment due to self-grown volume strain; and $\{\Delta P_n^s\}^e$ is the nodal load increment due to dry-shrinkage strain.

The following overall equilibrium equation can be established.

$$[K]^e \{\Delta\delta_n\}^e = \{\Delta P_n^c\}^e + \{\Delta P_n^T\}^e + \{\Delta P_n^g\}^e + \{\Delta P_n^s\}^e \tag{16}$$

Solution of Eq. (10) yields $\{\Delta\delta_n\}$, and then the stress increment $\{\Delta\sigma_n\}$ can be determined. Such that the total stress at time t_n can be obtained by accumulating stress increments of the time intervals.

$$\{\sigma_n\} = \{\Delta\sigma_1\} + \{\Delta\sigma_2\} + ... + \{\Delta\sigma_n\} = \sum_{i=1}^{n} \Delta\sigma_i \tag{17}$$

Sensitivity analysis method

To determine the most sensitive temperature control measures, and to optimize the temperature control scheme, a sensitivity analysis (SA) method is applied in this research as follows.

(1) Selection of influence factors and analysis indicators. Prior to conducting a sensitivity analysis, influence factors that tend to have the greatest impact on the temperature control of a concrete dam should be selected. Three temperature control measures are selected here as influence factors: concrete placement temperature, water-pipe cooling time, and thermal insulation layer thickness. Two distinct evaluations are selected as analysis indicators: the maximum temperature T^{max} and the maximum tensile stress O^{max}.

(2) Calculate the sensitivity indicators. The extent to which analysis indicators change owing to changes in the influence factors are taken as sensitivity indicators, where a sensitivity indicator represents the independent influence of each influence factor (*IF*). The general principle for evaluating the influence of an *IF* on the temperature control effect is based on the change in T^{max} (ΔT_{IF}^{k}) and the change in O^{max} ($\Delta\sigma_{IF}^{k}$) of the *k-th IF* (*k* = 1, 2, 3) according to the following formulas.

$$\Delta T_{IF}^{k} = \left| \frac{T_i^{\max} - T_j^{\max}}{IF_i^k - IF_j^k} \right| \tag{18}$$

$$\Delta\sigma_{IF}^{k} = \left| \frac{\sigma_i^{\max} - \sigma_j^{\max}}{IF_i^k - IF_j^k} \right| \tag{19}$$

Here, indices *i* (*i* = 1, 2, 3, 4, 5, 6, 7) and *j* (*j* = 1, 2, 3, 4, 5, 6, 7) denote the temperature control schemes that are being compared; $T_i^{\max}$ and $T_j^{\max}$ represent the maximum temperatures obtained for the corresponding temperature control schemes; $\sigma_i^{\max}$ and $\sigma_j^{\max}$ represent the maximum tensile stresses obtained for the corresponding temperature control schemes; and IF_i^k and IF_j^k are the values of the *k-th IF* of the corresponding temperature control schemes.

(3) Analyze the calculation results. The greater the values of ΔT_{IF}^{k} and $\Delta\sigma_{IF}^{k}$, the greater the sensitivity level of the corresponding *IF*.

CASE STUDY

Calculation model and coordinate system

A typical overflow dam monolith of an RCC gravity dam located in southwestern China is taken as the research object. The foundation elevation of the dam is 3,328 m and the crest elevation is 3,421 m. The height of the block is 93 m and the width is 20.5 m. The depth of the dam foundation is 100 m, the length from the heel to the upstream boundary is 100 m, and the length from the toe to the downstream boundary is 100 m as well.

The computational model and coordinate system of the dam monolith are shown in Figure 2. Eight-node hexahedral isoparametric elements are employed in the numerical model. The total number of elements is 20,190. The direction along which the river flows represents the positive x-axis direction and the vertical upward direction represents the positive z-axis direction. The remaining positive y-axis direction is placed to form a standard right-hand Cartesian coordinate system.

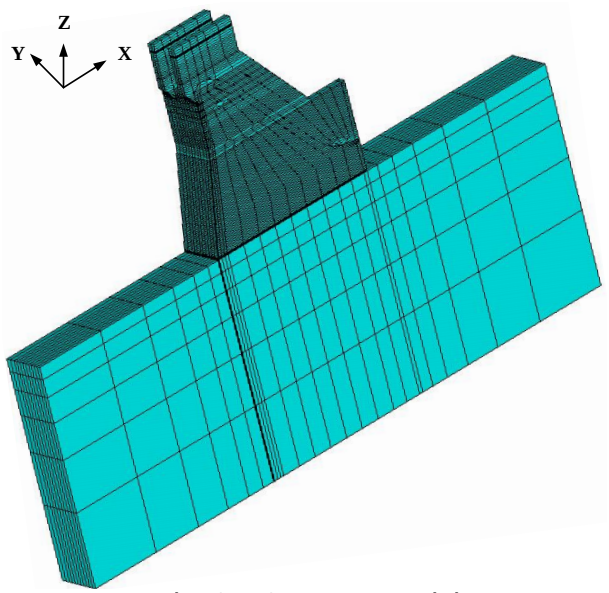

Fig. 2. - 3D FEM model

Basic parameters

Climate and material properties

Table 1 lists the air temperature and rock ground temperature of the dam site employed in the calculations. The annual and monthly average air temperatures are selected to obtain a cosine function that can approximate the air temperature of each day. The air temperature fitting function can be expressed as follows.

$$T_a = 8.6 + 8.5 \times \cos[2\pi \times (\tau - 210) / 365] \tag{20}$$

The material parameters of concrete mixtures for the dam monolith are listed in Table 2. The primary material properties of the dam and rock ground are listed in Table 3. Five types of concrete are employed in the dam block model, as shown in Figure 3. The adiabatic temperature rise of the concrete is a significant parameter in the simulation process. The adiabatic temperature rise of the five types of concrete and the corresponding calculation formulas are listed in Table 4, which were obtained under laboratory conditions. The equivalent surface heat transfer coefficients of the dam with 5 cm and 10 cm thick heat preservation quilts are 9.16 kJ/(m^2·h·°C) and 4.38 kJ/(m^2·h·°C), respectively.

Tab. 1. - The monthly average temperature values employed in the calculations

Month	1	2	3	4	5	6	7	8	9	10	11	12	Annual average
Air temper-ature (°C)	−0.7	2.6	6.5	10	12.9	14.5	16.2	15.8	12.9	8.9	3.6	−0.6	8.6
Rock ground temper-ature (°C)	0.3	4.8	9.8	13.6	17.3	18.8	19.8	19.9	15.8	11.7	5.5	0.2	11.5

Tab. 2. - The material parameters of concrete mixtures

Concrete	Gradation	Water-Cement Ratio	Material Dosage（kg/m^3）						
			Water	Cement	Fly Ash	Sand	Boulder	Mid Stone	Small Stone
$C_{90}20$ (distorted concrete)	2	0.45	531	708	472				
$C_{90}20$ (RCC)	2	0.50	102	102	102	757	0	807	538
$C_{90}15$ (RCC)	3	0.53	92	69.4	104.2	691	440	587	440
$C_{90}20$ (NC)	3	0.55	125	159.1	68.2	589	433	577	433
$C_{28}40$ (NC)	2	0.35	135	318.8	56.3	545	0	801	534

Tab. 3. - The thermal and structural properties of the dam and rock ground employed in the calculations

Materials		Temperature diffusivity (m^2/h)	Temperature conductivity (kJ/(m·h·°C))	Specific heat (kJ/(kg·°C))	Linear expansion coefficient (10^{-6}/°C)	Density (kg/m^3)	Standard elastic modulus (GPa)
Concrete	$C_{90}20$ (distorted concrete)	0.0037	8.18	0.926	9.01	2345	21.4
	$C_{90}20$ (RCC)	0.0038	8.10	0.921	8.95	2350	22.0
	$C_{90}15$ (RCC)	0.0038	8.30	0.912	9.06	2400	20.5
	$C_{90}20$ (NC)	0.0037	8.36	0.955	9.18	2390	23.4
	$C_{28}40$ (NC)	0.0039	8.55	0.934	9.40	2345	22.0
Rock ground		0.0038	8.10	0.902	8.5	2700	20

Tab. 4. - The adiabatic temperature rises and the corresponding calculation formulas

Concrete	Adiabatic temperature rise of concrete at different ages (°C)								Fitting calculation formulas
	1 d	3 d	5 d	7 d	10 d	14 d	21 d	28 d	
$C_{90}20$ (distorted concrete)	10.6	15.9	19.2	21.6	24.0	25.5	27.1	27.5	$\theta(\tau)=30.0d/(d+2.5)$
$C_{90}20$ (RCC)	6.0	11.2	14.3	16.3	18.8	20.4	21.5	22.0	$\theta(\tau)=24.9d/(d+3.4)$
$C_{90}15$ (RCC)	4.5	8.6	11.2	13.4	15.6	17.1	18.2	18.8	$\theta(\tau)=21.8d/(d+4.3)$
$C_{90}20$ (NC)	11.5	18.5	22.3	24.5	25.8	26.2	26.7	27.1	$\theta(\tau)=28.5d/(d+1.4)$
$C_{28}40$ (NC)	20.5	29.5	34.1	36.8	37.5	38	38.2	38.4	$\theta(\tau)=39.7d/(d+0.8)$

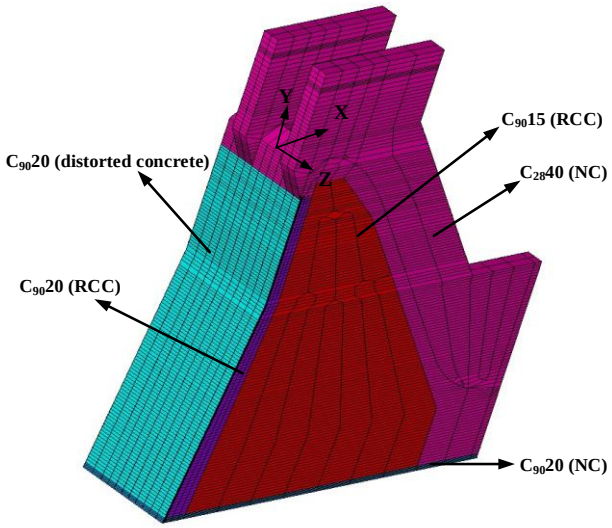

Fig. 3. - Material partition figure of the 3-D FEM dam block model

Temperature control criteria

According to the specification developed in China given in Design Specification for Concrete Gravity Dams (SL319-2005), the allowable temperature stress of concrete under the condition of uniform cooling can be estimated according to the concrete ultimate tensile strain by the following equation:

$$\gamma_0\sigma \le \varepsilon_p E_c / \lambda_{d3}, \tag{21}$$

where σ is the allowable tensile stress of concrete (MPa); ε_p is the standard value of the concrete ultimate tensile strain; E_c is the standard value of the concrete elastic modulus (GPa); γ_0 is the structure importance coefficient, which is set as 1.0; and λ_{d3} is the structure coefficient under the serviceability limit states, which is set as 1.5.

The detailed parameters and the values of σ for the five types of concrete at a given age are listed in Table 5. The maximum temperature of a concrete dam should be less than or equal to the specification limit of 29 °C.

Tab. 5: Allowable tensile stresses of the five types of concrete

Concrete / Parameters	C90 20 (distorted concrete)	C90 20 (RCC)	C90 15 (RCC)	C90 20 (NC)	C28 40 (NC)
Standard elastic modulus E_c (GPa)	21.4	22.0	20.5	23.4	22.0
Ultimate tensile strain ε_p (10^{-4})	0.88	0.88	0.90	0.78	1.20
Structural or safety coefficient λ_{d3}	1.5	1.5	1.5	1.5	1.5
Allowable tensile stresses σ (MPa)	1.29	1.29	1.40	1.07	1.76

Boundary conditions and calculation schemes

The bottom surface of the rock ground is added the annual average ground temperature load, and it is fully constrained. The upstream and downstream surfaces and left and right surfaces of the rock ground are thermally adiabatic, and are considered in the second boundary condition. Vertical constraints are also applied. The dam surface, which is exposed to air, is regarded as the third boundary condition in this calculation.

The HDPE pipe was used in this project to cool the concrete. Layout of water cooling pipes is shown in Figure 4. Basic material parameters of the pipe are listed in Table 6. The water temperature is 10 °C for all 7 schemes. Equivalent thermal diffusivity coefficients a' of concrete are used in the calculation process of this study. The equation of a' can be expressed as follows [12]:

$$a' = 1.947(a_1 b)^2 a, \tag{22}$$

where $a_1 b$ is the characteristic root of non-metallic cooling pipe which can be obtained from the Table 23-2-1 in the reference [12], a is the thermal diffusivity coefficient of concrete.

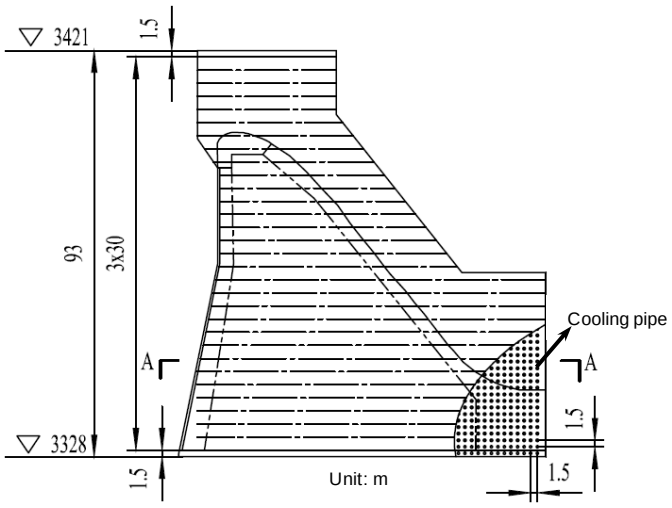

(a) Longitudinal profile of the cooling pipes layout

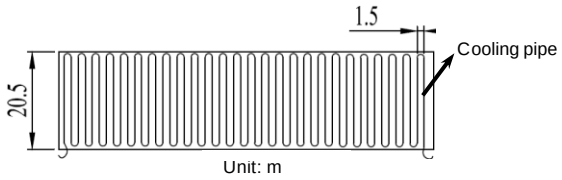

(b) Layout of the cooling pipes in cross section A-A

Fig. 4. - Layout of water cooling pipes

Tab. 6. - Basic material parameters of the HDPE cooling pipe

Parameters	Thermal diffusivity coefficient (W/(m×℃))	Pipe spacing (m×m)	Single pipe length (m)	Diameter (mm)	Thickness of the pipe wall (mm)
Value	≥0.45	1.5×1.5	≤250	32	2

The elastic modulus of different concrete mixtures was not constant during the simulation process. Hyperbolic type function was used to calculate the concrete elastic modulus at any age in this study. The equation can be expressed as follows [12].

$$E(\tau) = E_c \tau / (q + \tau) \tag{23}$$

where τ is the concrete age (d); $E(\tau)$ is the concrete elastic modulus at age τ ; E_c is the standard value of the concrete elastic modulus (GPa); q is a constant.

R is the solar heat absorbed by concrete surface (W/m^2); β is the surface conductance (kJ/(m^2·h·°C)); α_s is the absorption coefficient, given as 0.65 for concrete surface; S is the solar heat radiation on the concrete surface per unit area per unit time (kJ/(m^2·h)).

To analyse the degrees to which the concrete placement temperature, water-pipe cooling time, and thermal insulation layer thickness influence the temperature control effect during the construction of an RCC gravity dam, seven comparison schemes are proposed in this paper, which are listed according to their scheme number in Table 7. The initial placement time is set as July 1 of the first year in the simulation process. 32 lifts are contained and the interval time of adjacent placing layers is 10 d and the lift thickness is 3 m. The total simulation time is 791 d. Because the monthly average air temperature from early October to the end of April of the following year is below 10 °C, the surface heat preservation measure should be applied during this period.

Impact of solar radiation on the concrete temperature equals to air temperature increased ΔT_a, which is given as

$$\Delta T_a = \frac{R}{\beta} = \frac{\alpha_s S}{\beta} \tag{24}$$

where R is the solar heat absorbed by concrete surface (W/m^2); β is the surface conductance (kJ/(m^2·h·°C)); α_s is the absorption coefficient, given as 0.65 for concrete surface; S is the solar heat radiation on the concrete surface per unit area per unit time (kJ/(m^2·h)).

In this study, average β value of five kinds of concrete is adopted. $\beta=(\beta_1+\beta_2+\beta_3+\beta_4+\beta_5)/5=(8.18+8.10+8.30+8.36+8.55)/5=8.3$. S is obtained with monitoring equipment, given as 38.3 kJ/(m^2·h). So, an increase in ambient temperature of 3 °C is obtained based on Eq. 24. It is used to simulate the influence of solar radiation on the temperature field of the concrete surface during the construction of the RCC gravity dam.

Analysis type I consists of schemes 1, 2, and 3, which are designed for conducting the sensitivity analysis of the placement temperature. Analysis type II consists of schemes 1, 4, and 5, which are designed for conducting the sensitivity analysis of the water-pipe cooling time. Finally, Analysis type III consists of schemes 1, 6, and 7, which are designed for conducting the sensitivity analysis of the thermal insulation layer thickness.

Tab. 7. - Temperature control schemes

Analysis type	Scheme number	Placement temperature (°C)	Water-pipe cooling time (d)	Thermal insulation layer thickness (cm)
I	1	12	15	10
	2	15	15	10
	3	20	15	10
II	1	12	15	10
	4	12	20	10
	5	12	25	10
III	1	12	15	10
	6	12	15	5
	7	12	15	no heat preservation

Results and discussion

As the temperature field and stress field are time-varying values, the final simulation step is selected as typical time in this paper to carry out the sensitivity analysis as follows. Figure 5 shows the temperature contours of the dam block elements on the final simulation step for the seven temperature control schemes.

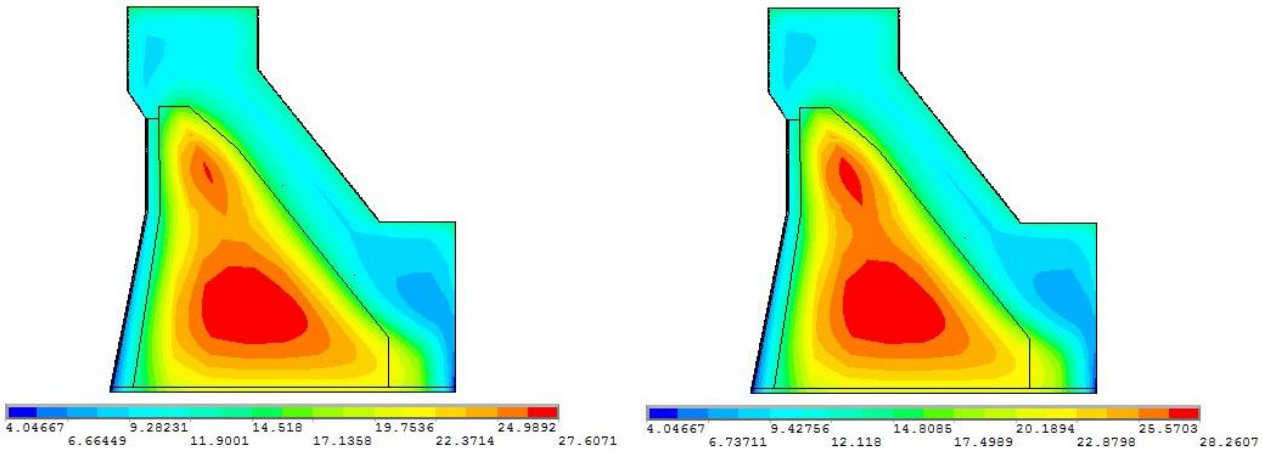

(a) (b)

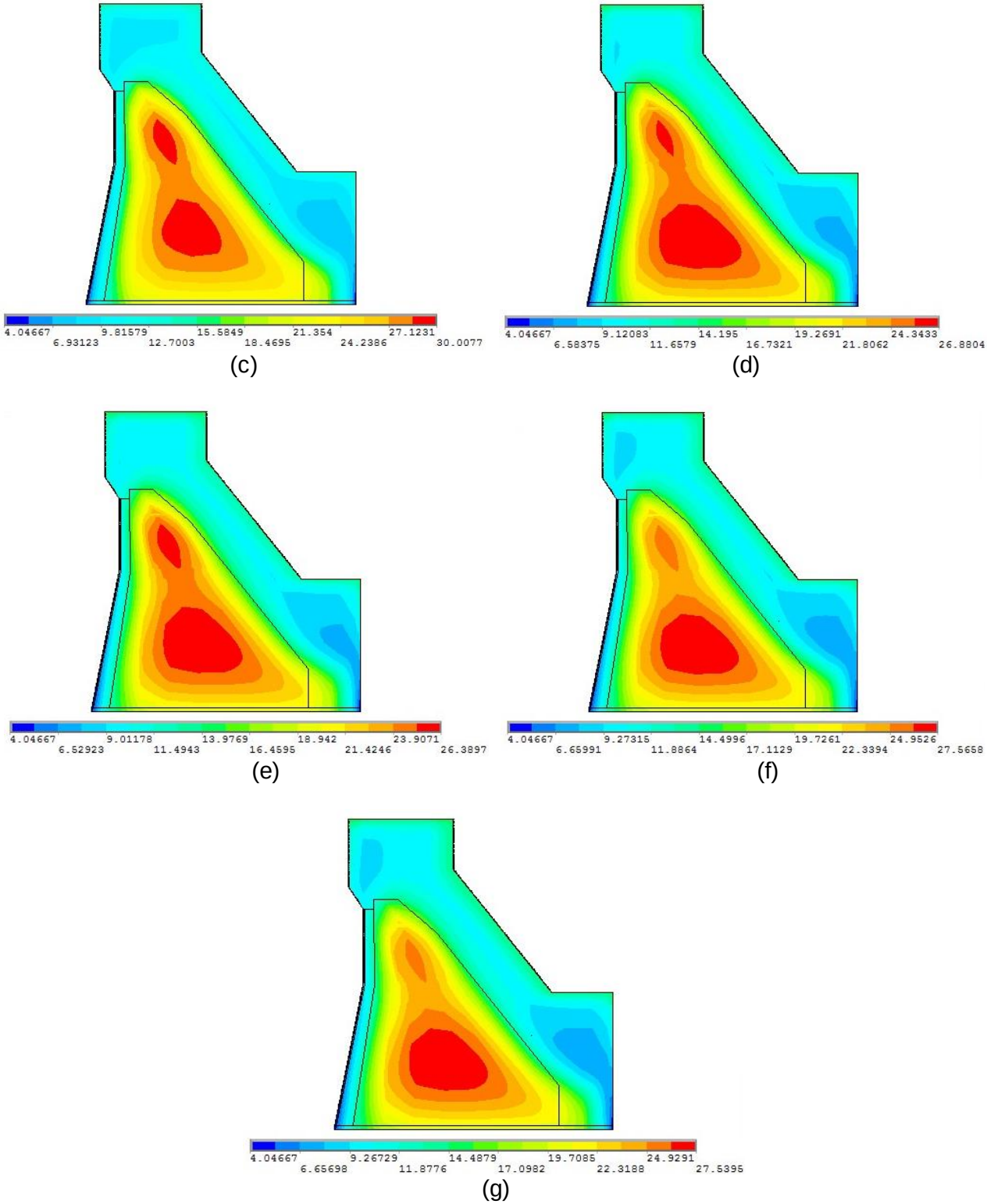

Fig. 5. - Temperature distributions of each temperature control scheme at the final simulation step (unit: °C): (a) Scheme 1, (b) Scheme 2, (c) Scheme 3, (d) Scheme 4, (e) Scheme 5, (f) Scheme 6, and (g) Scheme 7.

Sensitivity analysis of placement temperature

Schemes 1, 2, and 3 of Analysis type I employ placement temperatures of 12 °C, 15 °C, and 20 °C, respectively, as shown in Table 7. The water-pipe cooling times and thermal insulation layer thicknesses in these three schemes are fixed at 15 d and 10 cm, respectively.

From the temperature distributions of the dam block elements shown in Figures 5 (a), (b), (c), it can be seen that the maximum temperatures of schemes 1, 2, and 3 at the final simulation step are 27.61 °C, 28.26 °C, and 30.01 °C, respectively. The simulation results are listed in Tables 8. The boldfaced values in the table represent values that exceed the specification limits. When the placement temperature was increased from 12 °C to 15 °C, the maximum temperature of the dam increased by about 0.65 °C and ΔT_{IF}^{1} is 0.2167. Meanwhile, the maximum tensile stress increased by about 0.2 MPa and $\Delta \sigma_{IF}^{1}$ is 0.067. When the placement temperature was increased from 15 °C to 20 °C, the maximum temperature increased by about 1.76 °C and ΔT_{IF}^{1} is 0.35, whereas the maximum tensile stress increased by about 0.12 MPa and $\Delta \sigma_{IF}^{1}$ is 0.24.

The calculation results demonstrate that placement temperatures of 12 °C and 15 °C meet the requirements of temperature and stress control. When the placement temperature is increased to 20 °C, the maximum temperature and tensile stress of the dam block elements both exceed the specification limits.

According to the ΔT_{IF}^{1} and $\Delta \sigma_{IF}^{1}$ values obtained, it can be concluded that the placement temperature has a significant influence on the maximum temperature and tensile stress of the dam, and the placement temperature cannot exceed 15 °C. For safety considerations, the placement temperature should be 12 °C.

Tab. 8. - The maximum temperatures and stresses of the dam model at the final simulation step with different placement temperatures

Scheme number	Placement temperature (°C)	Maximum temperature (°C)	ΔT_{IF}^{1} (°C)	Maximum tensile stress (MPa)	$\Delta \sigma_{IF}^{1}$ (MPa/°C)	Allowable tensile stresses (MPa)
1	12	27.61	—	0.86	—	1.07
2	15	28.26	0.2167	1.06	0.067	1.07
3	20	**30.01**	0.35	**1.18**	0.24	1.07

Sensitivity analysis of water-pipe cooling time

Schemes 1, 4, and 5 of Analysis type II employ water-pipe cooling times of 15 d, 20 d, and 25 d, respectively, as shown in Table 7. The placement temperatures and thermal insulation layer thicknesses are fixed at 12 °C and 10 cm, respectively.

From the temperature distribution of the dam block elements shown in Figures 5 (a), (d), and (e), it can be seen that the maximum temperatures of schemes 1, 4, and 5 are 27.61 °C, 26.88 °C, and 26.39 °C, respectively. The simulation and sensitivity analysis results are listed in Table 9. The boldfaced value in the table indicates that the stress exceeds the specification limit. When the water-pipe cooling time was increased from 15 d to 20 d, the maximum temperature of the dam decreased by about 0.73 °C and ΔT_{IF}^{2} is 0.146. Meanwhile, the maximum tensile stress increased by about 0.12 MPa and $\Delta \sigma_{IF}^{2}$ is 0.024. When the water-pipe cooling time was increased from 20 d to 25 d,

the maximum temperature decreased by about 0.49 °C and ΔT_{IF}^2 is 0.098, whereas the maximum tensile stress increased by about 0.14 MPa and $\Delta \sigma_{IF}^2$ is 0.028.

The calculation results show that water-pipe cooling times of 15 d, 20 d, and 25 d all meet the requirements of temperature control. However, the maximum tensile stress of the dam block elements exceeds the specification limit for a water-pipe cooling time of 25 d.

According to the values of ΔT_{IF}^2 and $\Delta \sigma_{IF}^2$ obtained, it can be concluded that the water-pipe cooling time has a small influence on the maximum temperature, but has a substantial influence on the maximum tensile stress of the dam, and the water-pipe cooling time cannot exceed 20 d.

Tab. 9: The maximum temperatures and stresses of the dam model and value of sensitivity indicators with different water-pipe cooling times

Scheme number	Water-pipe cooling time (d)	Maximum temperature (°C)	ΔT_{IF}^2 (°C/d)	Maximum tensile stress (MPa)	$\Delta \sigma_{IF}^2$ (MPa/d)	Allowable tensile stresses (MPa)
1	15	27.61	—	0.86	—	1.07
4	20	26.88	0.146	0.98	0.024	1.07
5	25	26.39	0.098	**1.12**	0.028	1.07

Sensitivity analysis of thermal insulation layer thickness

Schemes 1, 6, and 7 of Analysis type III employ thermal insulation layer thicknesses of 10 cm, no heat preservation (i.e., 0 cm), and 5 cm, respectively. The placement temperature and water-pipe cooling time are fixed at 12 °C and 15 d, respectively.

From the temperature distributions of the dam block elements shown in Figures 5(a), (f), and (g), it can be seen that the maximum temperatures of the three schemes are 27.61 °C, 27.54 °C, and 27.57 °C, respectively. The boldfaced values in the table represent stress values that exceed the specification limit. When the thermal insulation layer thickness was decreased from 10 cm to no heat preservation, the maximum temperature of the dam decreased by about 0.07 °C and ΔT_{IF}^3 is 0.014. Meanwhile, the maximum tensile stress increased by about 1.37 MPa and $\Delta \sigma_{IF}^3$ is 0.614. When the thermal insulation layer thickness was increased from no heat preservation to 5 cm, the maximum temperature increased slightly and ΔT_{IF}^3 is 0.001, whereas the maximum tensile stress decreased by about 0.85 MPa and $\Delta \sigma_{IF}^3$ is 0.381. The simulation and sensitivity analysis results are listed in Table 10.

The calculation results show that thermal insulation layer thicknesses of 10 cm, no heat preservation, and 5 cm all meet the requirements of temperature control. However, with a thermal insulation layer thickness of 5 cm or no heat preservation, the maximum tensile stress of the dam block elements exceeds the specification limit.

According to the values of ΔT_{IF}^3 and $\Delta \sigma_{IF}^3$ obtained, it can be determined that the thermal insulation layer thickness has a small influence on the maximum temperature, but has a substantial influence on the maximum tensile stress of the dam, and the thermal insulation layer thickness should be 10 cm for surface heat preservation.

Tab. 10: The maximum temperatures and stresses of the dam model and value of sensitivity indicators with different thermal insulation layer thicknesses

Scheme number	Thermal insulation layer thickness (cm)	Maximum temperature (°C)	ΔT_{IF}^{3} (°C/ cm)	Maximum tensile stress (MPa)	$\Delta \sigma_{IF}^{3}$ (MPa/cm)	Allowable tensile stresses (MPa)
1	10	27.61	—	0.86	—	1.07
6	5	27.57	0.001	**1.38**	0.381	1.07
7	no heat preservation	27.54	0.014	**2.23**	0.614	1.07

CONCLUSIONS

An effective combination of temperature control measures is critical in the construction organization design of an RCC gravity dam. Based on the above study, the following conclusions can be drawn.

(1) An optimized temperature control scheme can be obtained by coupling 3-D FEM simulation of the thermal and stress distributions of concrete dams with the proposed sensitivity analysis method.

(2) The placement temperature has a substantial influence on the maximum temperature and tensile stress of the dam, and the placement temperature cannot exceed 15 °C.

(3) The water-pipe cooling time has a small influence on the maximum temperature, but has a substantial influence on the maximum tensile stress of the dam, and the water-pipe cooling time cannot exceed 20 d.

(4) The thermal insulation layer thickness has a small influence on the maximum temperature, but has a substantial influence on the maximum tensile stress of the dam. With a thermal insulation layer thicknesses of 10 cm, the maximum tensile stress can be controlled under the specification limit.

Taken together, according to the findings of the present study, the concrete temperature control measures are most effective when the placement temperature is 12 °C, the water-pipe cooling time is 20 d, and the thermal insulation layer thickness is 10 cm.

ACKNOWLEDGEMENTS

This research was supported by the National Natural Science Foundation of China (Grant No. 51479103), the Open Foundation of Key Laboratory of Hydropower Engineering Construction and Management of Hubei Province (Grant No. 2014KSD06). The authors thank the reviewers for useful comments and suggestions that helped to improve the paper. The authors would like to thank LetPub (www.letpub.com) for its linguistic assistance during the preparation of this manuscript.

REFERENCES

[1] Jing X. Y., Zhou W., Liu J. and Chang, X. L., 2013. Dynamic control measures of concrete temperature in rapid construction of high RCC dams. Engineering Journal of Wuhan University, vol. 46: 99-104.

[2] Zhang L., Liu Y., Li B. Q., Zhang G. X. and Zhang S. T., 2015. Study on Real-Time Simulation Analysis and Inverse Analysis System for Temperature and Stress of Concrete Dam. Mathematical Problems in Engineering, vol. 2015: 1-8.

[3] Chen Y. L., Wang C. J., Li S. Y., Wang R. J. and He J., 2001. Simulation analysis of thermal stress of RCC dams using 3-D finite element relocating mesh method. Advances in Engineering Software, vol. 32: 677-682.

[4] Malkawi A. I. H., Mutasher S. A. M. and Qiu T. J., 2003. Thermal-Structural Modeling and Temperature Control of Roller Compacted Concrete Gravity Dam. Journal of Performance of Constructed Facilities, vol. 17: 177-187.

[5] Xie H. W., Chen Y. L., 2005. Determination of the type and thickness for impervious layer in RCC dam. Advances in Engineering Software, vol. 36: 561-566.

[6] Noorzaei J., Bayagoob K. H., Thanoon W. A. and Jaafar M. S., 2006. Thermal and stress analysis of Kinta RCC dam. Engineering Structures, vol. 28: 1795-1802.

[7] Jaafar M. S., Bayagoob K. H., Noorzaei J. and Thanoon W. A. M., 2007. Development of finite element computer code for thermal analysis of roller compacted concrete dams. Advances in Engineering Software, vol. 38: 886-895.

[8] Chen S. H., Su P. F and Shahrour I., 2011. Composite element algorithm for the thermal analysis of mass concrete: Simulation of lift joint. Finite Elements in Analysis and Design, vol. 47: 536-542.

[9] Teixeira De Freitas J. A., Cuong P. T., Faria R. and Azenha M., 2013. Modelling of cement hydration in concrete structures with hybrid finite elements. Finite Elements in Analysis and Design, vol. 77: 16-30.

[10] Su H. Z., Li J. Y. and Wen Z. P., 2014. Evaluation of Various Temperature Control Schemes for Crack Prevention in RCC Arch Dams During Construction. Arabian Journal for Science and Engineering, vol. 39: 3559-3569.

[11] Gaspar A., Lopez-Caballero F., Modaressi-Farahmand-Razavi A. and Gomes-Correia A., 2014. Methodology for a probabilistic analysis of an RCC gravity dam construction. Modelling of temperature, hydration degree and ageing degree fields. Engineering Structures, vol. 65: 99-110.

[12] Zhu B. F., 2012. Thermal Stresses and Temperature Control of Mass Concrete, Beijing: China WaterPower Press.